EMU: GENERATIVE PRETRAINING IN MULTIMODALITY

Quan Sun[1]* **Qiying Yu**[2,1]* **Yufeng Cui**[1]* **Fan Zhang**[1]* **Xiaosong Zhang**[1]*
Yueze Wang[1] **Hongcheng Gao**[1] **Jingjing Liu**[2] **Tiejun Huang**[1,3] **Xinlong Wang**[1]†

[1] Beijing Academy of Artificial Intelligence [2] Tsinghua University [3] Peking University

Code & Demo: `https://github.com/baaivision/Emu`

ABSTRACT

We present **Emu**, a multimodal foundation model that seamlessly generates images and text in multimodal context. This omnivore model can take in any single-modality or multimodal data input indiscriminately (*e.g.*, interleaved image, text and video) through a one-model-for-all autoregressive training process. First, visual signals are encoded into embeddings, and together with text tokens form an interleaved input sequence. **Emu** is end-to-end trained with a unified objective of classifying the next text token or regressing the next visual embedding in the multimodal sequence. This versatile multimodality empowers the leverage of diverse pretraining data sources at scale, such as videos with interleaved frames and text, webpages with interleaved images and text, as well as web-scale image-text pairs and video-text pairs. **Emu** can serve as a generalist multimodal interface for both image-to-text and text-to-image tasks, supporting in-context image and text generation. Across a broad range of zero-shot/few-shot tasks including image captioning, visual question answering, video question answering and text-to-image generation, **Emu** demonstrates superb performance compared to state-of-the-art large multimodal models. Extended capabilities such as multimodal assistants via instruction tuning are also demonstrated with impressive performance.

1 INTRODUCTION

With text corpus at massive scale, Large Language Models (LLMs) (Brown et al., 2020; Chowdhery et al., 2022; Touvron et al., 2023) with straightforward training objectives such as next-word-prediction learn to understand, reason, and generate text with unprecedented accuracy and fluency, paving the way for diverse real-life applications (Schulman et al., 2022) unthinkable a decade ago. Recent studies (Alayrac et al., 2022; Driess et al., 2023; Hao et al., 2022) further investigate Large Multimodal Models (LMMs) beyond LLMs. Flamingo (Alayrac et al., 2022) connects a powerful language model with a pretrained vision encoder and inserts learnable layers to capture cross-modality dependencies, demonstrating strong abilities in multimodal zero-shot and in-context learning. Recent works (Li et al., 2023b; Dai et al., 2023; Huang et al., 2023; Liu et al., 2023b; Zhu et al., 2023a; Ye et al., 2023; Li et al., 2023a; Gong et al., 2023) adopt this framework and build LMM by docking a vision encoder with an LLM.

The prevailing training objective in such LMMs is predicting the next text token (Alayrac et al., 2022; Hao et al., 2022; Huang et al., 2023; Zhu et al., 2023a; Liu et al., 2023b; Li et al., 2023a), typically with a frozen vision encoder and no supervision for the vision part, which highly restricts model capacity. Besides, these LMMs are mostly trained on image-text pairs or documents, while overlooking video data as a potential scalable source of interleaved multimodal data. Documents interleaved with images (*e.g.*, textbooks, webpages) provide an intuitive representation of complex concepts, and have proved to be effective in empowering models with multimodal in-context learning ability (Alayrac et al., 2022; Zhu et al., 2023b). Videos, which usually contain interleaved image frames and subtitles (Figure 3), are an abundant source of multimodal data that naturally contains dense visual signals and encodes stronger cross-modal correlations with text than regular multimedia

*Equal contribution. † Correspondence to *wangxinlong@baai.ac.cn*.

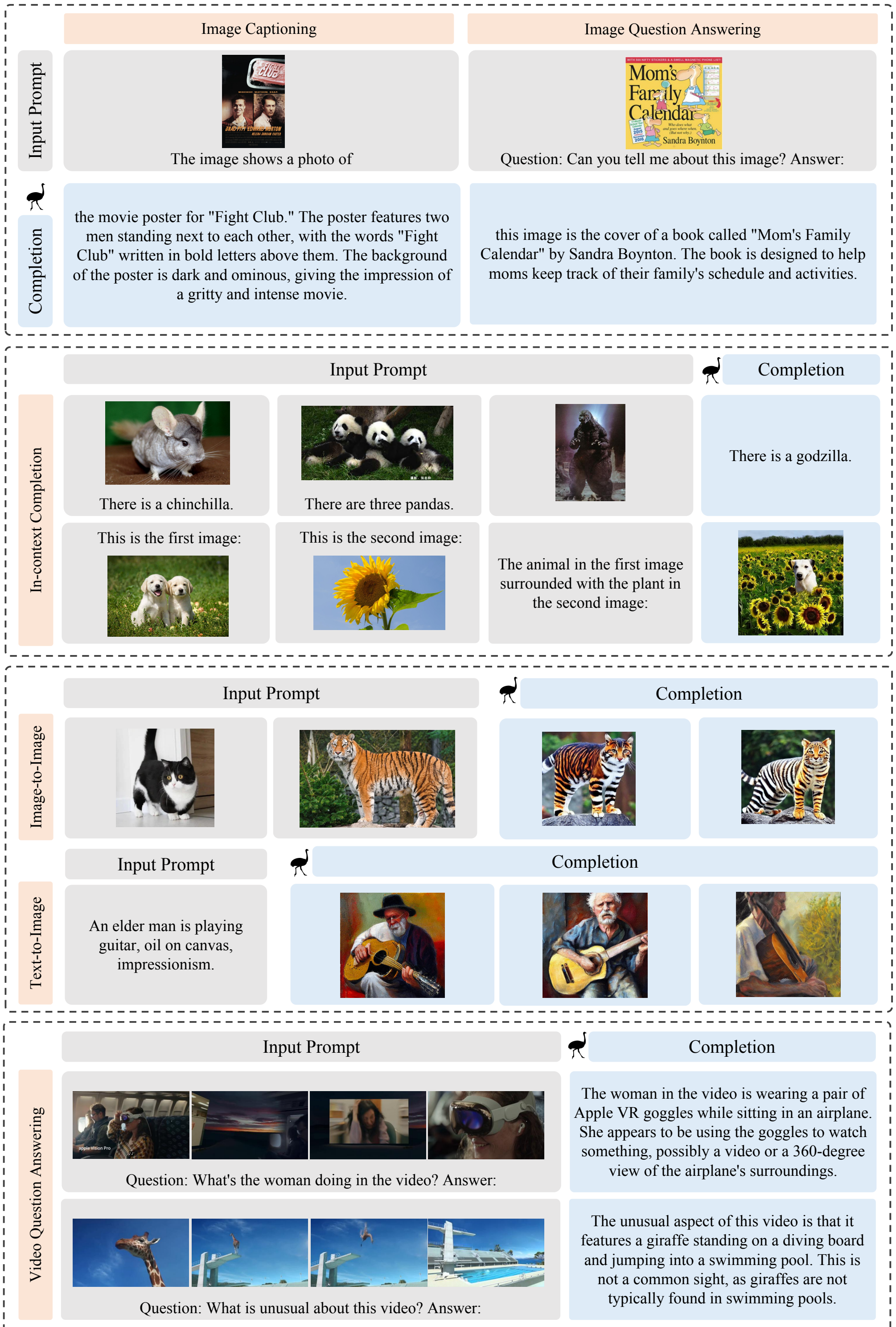

Figure 1: **Emu** as a generalist interface for diverse vision-language applications, such as image captioning, image/video question answering, in-context image-to-text and text-to-image generation, and image blending. More examples in Appendix E.

documents. Furthermore, public videos (especially user-generated clips) possess richer content diversity than Common Crawl[1], from which current training datasets mainly originate.

In this work, we introduce **Emu**, a large multimodal model that learns from both video and image data interleaved with text, under a unified objective of predicting the next visual or text token in an autoregressive fashion. To take advantage of rich web-scale data with an omnivore capacity, we formulate diverse sources of multimodal data (*e.g.*, videos with subtitles, webpages with images and text) into a unified format of interleaved image embeddings and text tokens (videos are converted into an interleaved sequence of randomly-selected frames and subtitles). Specifically, visual signals are first encoded into embeddings via a visual representation model EVA-CLIP (Sun et al., 2023), instead of being converted into discrete tokens. These visual embeddings together with text tokens constitute an interleaved multimodal input sequence, which will be fed into **Emu** for training.

We pretrain **Emu** on these multimodal data sequences under a simple unified objective: predicting the next element in a multimodal sequence. Different from existing LMMs that compute the predict-the-next loss on text tokens only, in training **Emu**, all input elements including both discrete text tokens and continuous image embeddings are accounted for loss computation. We adopt the cross-entropy classification loss for discrete text tokens, and the ℓ_2 regression loss for continuous visual embeddings. As raw images typically lack the left-to-right causal dependency as in language, **Emu** does not perform image generative pretraining in the original pixel space. Instead, visual embeddings are transformed into a causal latent space via Causal Transformer, which accepts the image encodings generated by EVA-CLIP as input, and outputs N tokens that capture the causal dependency of the given image (as illustrated in Figure 2).

Pretrained with the unified objective and diverse data forms, **Emu** can serve as a generalist interface for both image-to-text and text-to-image tasks by performing various types of completion in a multimodal sequence. As illustrated in Figure 1, **Emu** accepts multimodal prompts (*e.g.*, text, image, video, or their interleaved sequence) and generates multimodal response (for image generation, visual embeddings are decoded by a fine-tuned diffusion model). Further, **Emu** demonstrates impressive capabilities such as in-context text and image generation (the 2nd block of Figure 1), image blending (the 5th row of Figure 1 that combines a cat and a tiger into a real-looking tiger-cat), video understanding (the last block of Figure 1), and real-world knowledge grounding (Section 5.4).

We evaluate **Emu** on a broad range of zero-shot and few-shot tasks including image captioning, visual question answering, video question answering, and text-to-image generation. For qualitative demonstration, we also build an effective multimodal assistant via instruction tuning on multimodal conversational data. The instruction-tuned **Emu** assistant can effectively follow human instructions and interact with users via multimodal response.

2 EMU: PREDICT THE NEXT IN MULTIMODALITY

2.1 ARCHITECTURE

Emu is a large-scale multimodal model that performs completion in multimodality, *i.e.*, perceiving interleaved multimodal input and generating outputs varying in modalities. As illustrated in Figure 2, **Emu** consists of four parts: Visual Encoder, Causal Transformer, Multimodal Modeling, and Visual Decoder. We leverage pretrained EVA-CLIP (Sun et al., 2023), LLaMA (Touvron et al., 2023) and Stable Diffusion (Rombach et al., 2022) to initialize the Visual Encoder, the Multimodal Modeling LLM and the Visual Decoder, respectively.

Given any sequence of interleaved image, text and video, we first encode the image into dense visual features via EVA-CLIP, then transform the encodings into a fixed number of N visual causal embeddings via Causal Transformer. Similarly, we encode a video of T frames into $T \times N$ visual causal embeddings. Two special image tokens `[IMG]` and `[/IMG]` are prepended and appended for each image or frame, respectively, to represent the beginning and end of the encoded image/frame embeddings. The visual causal embeddings are combined with text tokens to form multimodal sequences that are fed into the Multimodal Modeling LLM for unified autoregressive modeling. We append `<s>` and `</s>` tokens to the start and the end of each sequence. In inference, we fine-tune the Visual Decoder to decode the visual embeddings into a realistic image.

[1]https://commoncrawl.org/

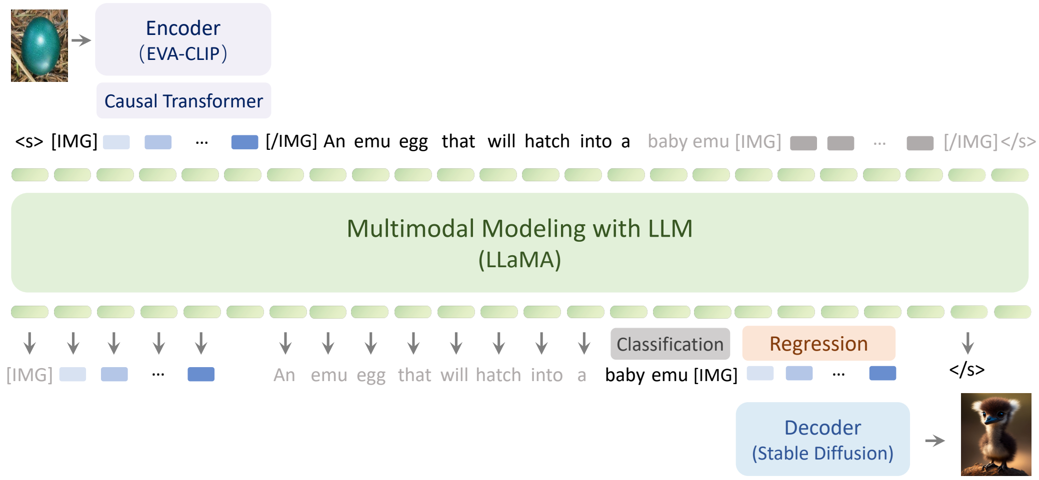

Figure 2: **Emu** unifies the modeling of different modalities in an auto-regressive manner. Visual signals are first encoded into embeddings, and together with text tokens form an interleaved sequence. The training objective is to either classify the next text token or regress the next visual embedding. In inference, regressed visual embeddings are decoded into a realistic image via a fine-tuned latent diffusion model.

Causal Transformer. Auto-regressively modeling images in raster order is counter-intuitive and has not demonstrated satisfactory performance, which may be attributed to the fact that images naturally possess 2D structures and are not perceived as sequential signals like text. To better capture the characteristics of images and achieve unified modeling of different modalities, we propose a Causal Transformer module to transform 2D spatial visual signals to 1D causal sequences in a latent space Z. Specifically, given an image I with its encodings $g(I)$ from EVA-CLIP as condition, Causal Transformer accepts randomly initialized embeddings $\{e_1, e_2, \dots, e_N\}$ as input, and outputs N embeddings $\{z_1, z_2, \dots, z_N\}$ that capture the causal dependency of the given image. The architecture of Causal Transformer is similar to the decoder of Transformer (Vaswani et al., 2017), with each block consisting of a causal self-attention layer, a cross-attention layer, and a feed-forward layer. The cross-attention layer aggregates visual information from the image embeddings extracted from EVA-CLIP, where the visual embeddings are treated as keys and values, and the outputs from the previous causal attention layer serve as queries.

Visual Decoder. We use a latent diffusion model to decode visual embeddings into images, and adopt the weights of Stable Diffusion (Rombach et al., 2022) for initialization. Specifically, we feed N visual embeddings generated by **Emu** into the diffusion model as conditions for image decoding. We replace the linear projections of the cross-attention modules in Stable Diffusion with new linear layers that accommodate the dimension of **Emu** and Stable Diffusion.

2.2 Training Objective

Given an unlabeled web-scale corpora $\mathcal{D}$ consisting of interleaved multimodal sequences $x = (x_1, x_2, \dots, x_n)$, where x can be vision-language sequences of various forms, such as image-text pairs, image-text interleaved documents, or videos with subtitles. x_i can be a signal unit (text or image token) from any arbitrary modality. We first convert all continuous 2D signals (images and video frames) into 1D causal latent embedding sequences using Causal Transformer, then insert them back into the corresponding places in the sequence x. The resulting sequence is represented as $u = (u_1, u_2, \dots, u_m)$, where u_i can be either a discrete text token, or a visual embedding that captures causal dependency with neighboring visual embeddings.

We approximate the likelihood of the web-scale corpora $p(x)$ with $p(u)$, and maximize the likelihood in a unified auto-regressive manner as follows:

$$\max_\theta \sum_{u \in \mathcal{D}} \sum_{i=1}^{|u|} \log P(u_i | u_1, \dots, u_{i-1}; \theta) \approx p(x) \tag{1}$$

Two types of losses are adopted to optimize this objective. For discrete text tokens, cross-entropy loss is used to supervise classification in the predefined vocabulary with a language modeling head. For continuous visual embeddings, ℓ_2 regression loss is adopted with a separate regression head.

2.3 GENERALIST INTERFACE

The unified auto-regressive modeling of different modalities endows **Emu** with a powerful ability to serve as a multimodal generalist that can perform any types of completion in a multimodal sequence, *i.e.*, accepting multimodal sequence as input, and outputting signals across vision and language modalities. For example, given two examples as the prompt, **Emu** automatically infers and completes the corresponding task given a new input, as shown in the second block of Figure 1.

Specifically, given a multimodal context, if the expected output format is text, **Emu** will use the language modeling head to generate discrete text tokens. If the desired output is image, we will append a `[IMG]` token at the end of the input sequence, then **Emu** will autoregressively generate N visual embeddings that will then be sent to the visual decoder for decoding into a real-world image.

3 EMU TRAINING

We pretrain **Emu** with web-scale data across modalities in various forms, including image-text pairs (LAION-2B (Schuhmann et al., 2022), LAION-COCO (lai, b)), interleaved images-text data (MMC4 (Zhu et al., 2023b)), video-text pairs (WebVid-10M (Bain et al., 2021)), and our collected interleaved video-text data (YT-Storyboard-1B). All these data are formulated as multimodal sequences, from which **Emu** learns under the objective of predict-the-next-element in a unified auto-regressive manner. After pretraining, we finetune a decoder to transform visual embeddings into realistic images.

3.1 DATA

Image-text Pairs. We use the image-text pairs from LAION-2B (Schuhmann et al., 2022) and LAION-COCO (lai, b) for pretraining. LAION-2B provides images paired with noisy alt-texts from the web, and LAION-COCO is its 600M subset that is captioned by BLIP (Li et al., 2022).

Video-text Pairs. WebVid-10M (Bain et al., 2021) is an extensive dataset consisting of a large collection of short videos with textual descriptions. These videos are sourced from materials websites with diverse contents and a strong correlation between text and video. We use heuristic rules to remove irrelevant metadata (*e.g.*resolution of the original video, camera parameters).

Interleaved Image and Text. Large-scale image-text interleaved data plays a crucial role in unlocking the in-context learning ability of multimodal models. We leverage the Multimodal-C4 (MMC4) dataset (Zhu et al., 2023b), an expanded version of the text-only C4 (Raffel et al., 2020). MMC4 comprises a collection of approximately 75 million image-text-interleaved documents, with 400 million images and 38 billion tokens in total. From each document, we sample a random subsequence of L = 1024 take up to the first N = 5 images. Additionally, we randomly sample N = 5 images along with their corresponding sentences to construct a subsequence of L = 512.,

Interleaved Video and Text. Videos with subtitles also present a promising and scalable source of interleaved multimodal data. We introduce the YT-Storyboard-1B dataset which collects 18 million videos and their corresponding subtitles from YouTube[2] using the video-ids provided by the YT-Temporal-1B dataset (Zellers et al., 2022). Instead of raw videos, we collect storyboard images (about 1.8 billion images in total), a set of thumbnails provided by the YouTube website for quick video viewing. The combination of storyboard thumbnails and subtitles creates a natural interleaved sequence of video and text ordered by timestamps, as in Figure 3. More details are in Appendix A.1.1.

3.2 PRETRAINING

We initialize **Emu**'s Visual Encoder with the 1B version of EVA-01-CLIP (Sun et al., 2023), and Multimodal Modeling LLM with the 13B version of LLaMA (Touvron et al., 2023). LLaMA is a decoder-only Transformer (Vaswani et al., 2017) and EVA-01-CLIP is a 40-layer ViT (Dosovitskiy

[2]`https://www.youtube.com`

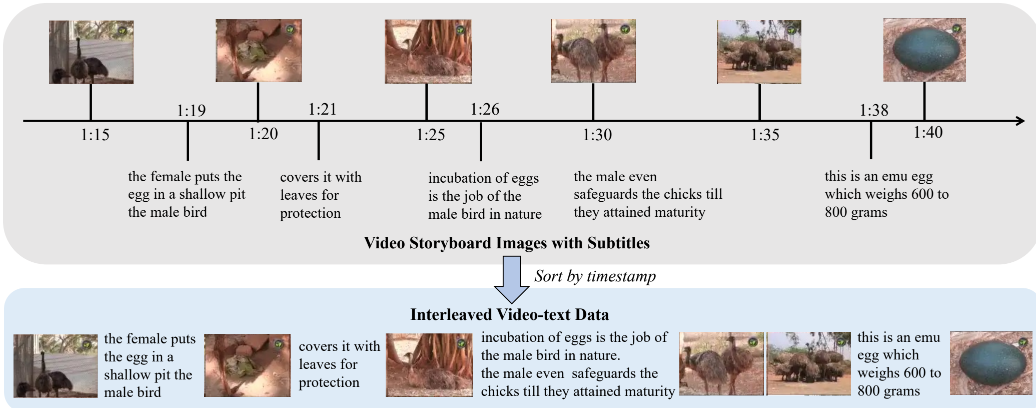

Figure 3: Interleaved video-text data. The combination of storyboard thumbnails and subtitles captions creates a natural interleaved sequence of video and text that is ordered by the timestamps.

et al., 2021). The Causal Transformer comprises 12 blocks, each of which consists of a causal self-attention layer, a cross-attention layer, and a feed-forward layer. Random initialization is used for Causal Transformer. The total number of parameters of **Emu** is 14B and is trained end-to-end.

We use a batch size of 128 for image-text pair data, 64 for interleaved image-text data, 16 for video-text pair and interleaved video-text data. Detailed pertaining hyperparameters are in Appendix A.1.1. For each video, we randomly sample 8 frames for pretraining, and all images/frames are resized into 224×224 resolution. For image-text pair and interleaved data, we randomly put each image before or after its corresponding sentence. We train the model on 128 NVIDIA 80G-A100 GPUs for 10k steps with around 82M samples (150B tokens in total), and the pretraining takes approximately 2 days.

3.3 Visual Decoding

After pretraining, we tune the visual decoder with both LAION-COCO (lai, b) and LAION-Aesthetics (lai, a) (a high-aesthetics quality subset of LAION-5B (Schuhmann et al., 2022)) image-text pair datasets under text-to-image task. Specifically, We initialize the diffusion model with Stable Diffusion v1.5. We freeze the Visual Encoder, Multimodal Modeling LLM in **Emu**, and the VAE in diffusion model during training, with only the parameters of U-Net updated. For each training sample, we append the `[IMG]` token to the end of the input text and feed it into the Multimodal Modeling LLM, which will then generate N visual embeddings in an auto-regressive manner. These visual causal embeddings are fed into Image Decoder as the condition for image generation training.

We follow the model setups of Stable Diffusion v1.5. We train the diffusion model with 32 A100-40G GPUs for 15k iterations. Detailed hyperparameters are in Appendix A.2. To further improve sample quality, we randomly drop image embeddings condition by 10% of the time during training to enable classifier-free guidance (Ho & Salimans, 2022).

4 Instruction Tuning

Language instruction tuning has helped pretrained language models to align with user intentions (Ouyang et al., 2022; Wang et al., 2022c; Taori et al., 2023; Zheng et al., 2023) and generalize to unseen tasks (Wei et al., 2022; Chung et al., 2022). We apply multimodal instruction tuning on **Emu** to align it with human instructions through supervised finetuning on publicly available datasets, including language instructions from ShareGPT (Zheng et al., 2023) and Alpaca (Taori et al., 2023), image-text instructions from LLaVA (Liu et al., 2023b), and video instructions from VideoChat (Li et al., 2023c) and Video-ChatGPT (Maaz et al., 2023). Dataset details can be found in Appendix B.1.

In instruction tuning, we freeze all parameters of pretrained **Emu**, and fine-tune a low-rank adaption (LoRA) module (Hu et al., 2022). The main focus of instruction tuning is to align the model with natural language instructions, which are less relevant to vision features. Thus, we attach LoRA modules only to the self-attention layers of the Multimodal Modeling LLM, and add no adaptation to the Vision Encoder. Training details can be found in Appendix B.1.

Table 1: Zero-shot comparison, * indicates that the zero-shot prompt is built by using two examples from the task, where their corresponding images have been removed. **Emu-I** is the instruction-tuned **Emu** model. The best results are **bold** and the second best are underlined.

Models	Image-Text Tasks							Video-Text Tasks		
	COCO	NoCaps	Flickr30K	VQAv2	OKVQA	VizWiz	VisDial	MSVDQA	MSRVTTQA	NExTQA
Per-task Finetuning										
PALI-X-55B	149.2	126.3	-	86.0	66.1	70.9	-	-	47.1	38.3
MetaLM	82.2	58.7	43.3	41.1	11.4	-	-	-	-	-
Kosmos-1	84.7	-	67.1	51.0	-	29.2	-	-	-	-
Flamingo-9B *	79.4	-	61.5	51.8	44.7	28.8	48.0	30.2	13.7	23.0
Emu	112.4	96.5	72.0	52.0	38.2	34.2	47.4	18.8	8.3	19.6
Emu *	-	-	-	52.9	42.8	34.4	47.8	34.3	17.8	**23.4**
Emu-I	**120.4**	**108.8**	**77.4**	57.2	43.4	32.2	43.0	34.6	16.8	5.8
Emu-I *	-	-	-	**62.0**	**49.2**	**38.3**	**51.1**	**37.0**	**21.2**	19.9

All instruction-tuning data are packed with this template:

$$\texttt{<System Message> [USER]: <Instruction> [ASSISTANT]: <Answer>,} \quad (2)$$

where [USER] and [ASSISTANT] are special tokens initialized from the embeddings of words 'user' and 'assistant', respectively. <System Message> varies depending on the specific task (Appendix B.2). <Instruction> and <Answer> are actual slots for human instructions and assistant answers, and only <Answer> is accounted for loss computation.

5 EVALUATION

We evaluate **Emu** on a broad range of vision-language tasks including image captioning (MS-COCO (Chen et al., 2015)), image question answering (VQAv2 (Goyal et al., 2017), OKVQA (Marino et al., 2019), VizWiz (Gurari et al., 2018)), visual dialog (VisDial (Das et al., 2017)), video question answering (MSRVTTQA (Xu et al., 2017), MSVDQA (Xu et al., 2017), NextQA (Xiao et al., 2021)) and text2image generation(MS-COCO (Lin et al., 2014)). Details are described in Appendix C.1. We evaluate our pretrained and instruction-tuned models in zero-shot and few-shot settings.

5.1 ZERO-SHOT EVALUATION

In the zero-shot setting, the model is tested on tasks and datasets never encountered during training. Task-specific prompts are used to indicate different tasks to perform, without any additional tuning for model parameters.

Multimodal Understanding. Table 1 presents the zero-shot multimodal understanding performance of **Emu** and **Emu-I** (the instruction-tuned model). For zero-shot evaluation of **Emu**, we adopt the multimodal Chain-of-Thought prompting technique following Huang et al. (2023), which first asks the model to generate a caption for visual content before outputting the final result. Additionally, we evaluate using the same strategy following Flamingo (Alayrac et al., 2022), where two text-only examples from the task are used as prompts (results indicated by an *). For more detailed information regarding the evaluation, please refer to Appendix C.2.

On COCO captioning task, **Emu** achieves impressive zero-shot CIDEr score (Vedantam et al., 2015) of 112.4, which outperforms other LMMs by a large margin. In a wide range of image and video question answering tasks, **Emu** consistently surpasses LMMs like Kosmos-1 and Flamingo-9B. Notably, **Emu** achieves an accuracy of 34.4% on the complex VizWiz VQA dataset, versus Kosmos-1's 29.2% and Flamingo-9B's 28.8%. **Emu-I** is the instruction-tuned **Emu** model that achieves notable improvements. Remarkably, even with only 14B parameters, **Emu-I** can outperform much larger-scale Flamingo-80B model in several tasks such as VQAv2 (62.0% vs. 56.3%), VizWiz (38.3% vs. 31.6%), and MSVDQA (37.0% vs. 35.6%).

Text2image Generation. We evaluate the zero-shot image generation ability on the validation set of MS-COCO (Lin et al., 2014). Following (Ramesh et al., 2021), we randomly sample 30k prompts from the validation set and calculate the zero-shot FID (Heusel et al., 2017). The results are shown in Table 2. For the generation of both **Emu** and SDv1.5, we use PNDM (Liu et al., 2022) scheduler with

Table 3: Few-shot comparison. k is the number of in-context examples, and we used the same example selection approach (*i.e*. RICES (Yang et al., 2022b)) as Flamingo (Alayrac et al., 2022).

Models	VQAv2			VizWiz			MSVDQA			MSRVTTQA		
	k=2	k=4	k=8	k=2	k=4	k=8	k=2	k=4	k=8	k=2	k=4	k=8
Kosmos-1	51.4	51.8	51.4	31.4	35.3	39.0	-	-	-	-	-	-
Flamingo-9B	-	56.3	58.0	-	34.9	39.4	-	36.2	**40.8**	-	18.2	23.9
PALI-X	-	56.9	57.1									
Emu	**56.4**	**58.4**	**59.0**	**37.8**	**41.3**	**43.9**	**36.0**	**37.1**	39.8	**21.2**	**21.8**	**24.1**

Table 4: Zero-shot evaluation regarding each core VL capability of MM-Vet (Yu et al., 2023b).

Model	Rec	OCR	Know	Gen	Spat	Math	Total
LLaMA-Adapter v2-7B (Gao et al., 2023)	16.8	7.8	2.5	3.0	16.6	4.4	13.6±0.2
MiniGPT-4-14B (Zhu et al., 2023a)	29.9	16.1	20.4	22.1	22.2	3.8	24.4±0.4
InstructBLIP-14B (Dai et al., 2023)	30.8	16.0	9.8	9.0	21.1	10.5	25.6±0.3
DreamLLM-7B (Dong et al., 2023)	41.8	26.4	33.4	33.0	31.0	11.5	35.9±0.1
LLaVA-65B (Lu et al., 2023)	39.2	**28.2**	26.2	28.3	**33.0**	**15.0**	35.5±0.3
Emu-I -14B	**45.5**	19.2	**36.7**	**35.9**	25.2	3.8	**36.3±0.3**

50 steps. We also adopt classifier-free guidance (Ho & Salimans, 2022) for better generation quality. The scaling factor is set to 5.0 and 3.0 for **Emu** and SDv1.5 respectively, as these settings yield the best performance for both models. **Emu** achieves better performance compared to a concurrent work GILL (Koh et al., 2023a), which also generates images with LLMs. However, our model is inferior to SDv1.5 in terms of FID. This is probably because the condition space (image embeddings) of our visual decoder deviates a lot from the condition space (text embeddings) of the diffusion model used as initialization, and our model is trained for a relatively short 15k steps.

5.2 Few-shot Evaluation

In few-shot evaluation, the model is prompted with task-specific prompts and several examples collected from the training data to evaluate its in-context learning ability. Evaluation details can be found in Appendix C.3. Table 3 presents the performance of the pretraining model **Emu** in image and video question answering tasks under the few-shot ($k = 2, 4, 8$) evaluation setting. We use the Retrieval In-Context Example Selection (Yang et al., 2022b) approach following Flamingo (Alayrac et al., 2022). **Emu** demonstrates superior performance to Flamingo-9B and Kosmos-1 under almost all scenarios. For example, **Emu** achieves a VQAv2 accuracy of 58.4% and VizWiz 41.3% under the 4-shot setting, surpassing Flamingo-9B by +2.1% and +6.4%, respectively. For video-text tasks, **Emu** demonstrates strong performance as well, such as 4-shot 21.8% v.s. Flamingo's 18.2% on the MSRVTTQA benchmark. Additionally, we can observe a positive correlation between the number of shots k ($k = 0, 2, 4, 8$) and the performance of **Emu**. These results demonstrate **Emu**'s remarkable in-context learning ability.

Table 2: Zero-shot text-to-image results on MS-COCO validation set. 30k samples are randomly sampled for evaluation.

Models	FID(↓)
unimodal generation models	
GLIDE (Nichol et al., 2021)	12.24
Make-A-Scene (Gafni et al., 2022)	11.84
DALL-E 2 (Ramesh et al., 2022)	10.39
SDv1.5 (Rombach et al., 2022)	9.93
Imagen (Saharia et al., 2022)	7.27
Parti (Yu et al., 2022b)	7.23
multimodal generation models	
GILL (Koh et al., 2023a)	12.20
Emu (ours)	**11.66**

5.3 In-the-wild Evaluation

Table 4 presents zero-shot evaluation results on the in-the-wild benchmark MM-Vet (Yu et al., 2023b). We report the mean and std of 5 evaluation runs following Yu et al. (2023b). For each core capability, the average score is reported. **Emu-I** exhibits state-of-the-art in-the-wild capability, and even outperforms LLaVA-65B (Lu et al., 2023) in Rec, Know, Gen abilities and the total score.

5.4 Qualitative Evaluation

Beyond quantitative benchmarks, we conduct adequate qualitative evaluation of **Emu**. **Emu** demonstrates impressive capabilities that cannot be evaluated on standard benchmarks, including real-world knowledge grounding (upper right of Figure 4), interleaved multi-image understanding (left side of Figure 4), detailed video understanding (lower right of Figure 4), multimodal assistant (Figure 5), multi-turn dialogue (Figure 6), image blending (Figure 7), and (in-context) text-to-image generation. For in-context text-to-image generation, **Emu** can generate context-related images (in the first two rows of Figure 8, the generated images share the oil painting style in context, compared with the corresponding images generated without context in the first two rows of Figure 9), and follow context-related instructions, as shown in the 4th row of Figure 1. The multimodal in-context ability of **Emu** is responsible for this brand-new ability of image generation.

We also compare **Emu** with other state-of-the-art multimodal assistants in terms of the ability to perform typical image captioning tasks (Figure 10) and follow human instructions (Figure 11). In Figure 11, we test a slightly difficult instruction, and only **Emu** response properly to list 8 books written by Agatha Christie and then recommend one.

6 Related Work

Multimodal pretraining (Radford et al., 2021; Jia et al., 2021; Sun et al., 2023; Chen et al., 2020; Kim et al., 2021; Wang et al., 2022d;a;b; Cho et al., 2021; Li et al., 2021; Yu et al., 2022a; Chen et al., 2023c; Lu et al., 2022) learns cross-modal interactions from large-scale multimodal data. Flamingo (Alayrac et al., 2022) bridges powerful yet private pretrained vision and large language models and first demonstrates remarkable multimodal zero-shot and few-shot behaviors. With the increasing impact (Schulman et al., 2022) and accessability (Touvron et al., 2023) of LLMs, recent work has also considered building multimodal models based on LLMs (Li et al., 2023b; Driess et al., 2023; Huang et al., 2023; Dai et al., 2023; Ye et al., 2023; Zeng et al., 2023; Koh et al., 2023b), such as BLIP-series (Li et al., 2023b; Dai et al., 2023) that connect frozen vision and language pretrained models with a Q-Former to bridge the modality gap. These LMMs commonly use predicting the next text token as the training objective and exert no supervision for vision data (Hao et al., 2022; Huang et al., 2023; Zhu et al., 2023a; Liu et al., 2023b; Ye et al., 2023). Instead, **Emu** unifies the modeling of vision and language with the objective of predicting the next visual or text token in an autoregressive manner, and further explores videos as a new source of interleaved image-text data. This unified modeling leads to a generalist interface for diverse multimodal tasks that output either image or text. Emerging recent studies (Zhu et al., 2023a; Liu et al., 2023b; Maaz et al., 2023; Li et al., 2023c; Liu et al., 2023a; Li et al., 2023a; Chen et al., 2023b;a) attempt to build powerful visual multimodal assistants based on LMMs through constructed conversation data. We also instruction-tune **Emu** using publicly available datasets and build a multimodal assistant that aligns well with human instructions on both images and videos.

7 Limitations and Future Topics

Emu shares the well-acknowledged constraints inherent in other LLMs and LMMs, including susceptibility to both visual and language hallucinations, slow auto-regressive inference speed, a cessation of knowledge updates after pretraining, and a potential for generating non-factual content. Besides, Emu predominantly focused on English-language data. As a result, the model's proficiency in languages other than English is currently delicate, and users should exercise caution when applying it in such contexts. Addressing challenges related to hallucination, enhancing inference speed, and expanding multilingual capabilities are crucial areas for future exploration and improvement.

8 Conclusion

In this work, we present **Emu**, a Large Multimodal Model trained with a unified autoregressive objective of predicting the next element, including both visual and textual tokens. Apart from commonly used image-text pairs and interleaved documents, we explore another scalable data source of image-text interleaved data, *i.e.*, video. **Emu** trained under such unified objective and diverse data can serve as a generalist interface that is capable of performing diverse multimodal tasks, such as image captioning, image/video question answering, and text-to-image generation, together with new abilities like in-context text and image generation, and image blending. We also build a multimodal assistant instruction-tuned on **Emu**, which exhibits excellent human-aligned abilities such as multi-turn dialogue. We hope that our work will inspire the community to continue exploring the potential of diverse multimodal data at web-scale and also the generative pretraining beyond vision and language.

ETHICS STATEMENTS

Emu is currently in a preliminary stage and has been developed solely for research purposes. Its usage in specific applications is not recommended until comprehensive risk analyses have been conducted and corresponding mitigation strategies thoroughly explored. The ensuing discussion outlines potential risks and corresponding mitigation strategies of Emu, acknowledging the necessity for further research efforts to comprehensively assess associated risks.

POTENTIAL RISKS

The ethical considerations associated with Emu primarily stem from two key aspects: 1) model initialization: the Multimodal Modeling module of Emu is initialized from an open-sourced large language model LLaMA (Touvron et al., 2023), the Visual Decoder module is initialized from Stable Diffusion (Rombach et al., 2022), and the Vision Encoder is initialized from EVA-CLIP (Sun et al., 2023). Consequently, Emu inherits the potential risks of generating harmful and biased information, including offensive language, propagation of social biases and stereotypes, and the generation of inappropriate content such as pornography and child abuse. 2) Pretraining data. The pretraining data of Emu are publicly available and they are sourced from the Internet, where bias and harmful information are prevalent. Besides, the datasets sourced from the Internet (such as Common Crawl) may include links to images with personal information, potentially compromising privacy and containing sensitive content like faces, medical images, or other personal data.

MITIGATION STRATEGIES

It is crucial to reiterate that Emu is designed exclusively for preliminary academic research and should not be deployed in specific applications without rigorous risk analyses and mitigation strategy exploration. Deployment in production environments warrants a more thorough investigation into model behavior and potential biases.

Given the extensive size of pre-training datasets and the associated training costs, curating datasets and developing models for widespread use exceeds the scope of a single research paper. However, we are open to discussing mitigation strategies to help address ethical concerns.

Short-term approaches include: 1) relying on prompting to mitigate any biases and harmful outputs, 2) implementing rule-based filtering, human oversight, and evaluation to identify and block harmful information, 3) employing a discriminator model capable of classifying harmful information for enhanced blocking, 4) Emu itself can be finetuned to become a multimodal discriminator.

In the long term, strategies involve: 1) social or public policy interventions, such as regulatory frameworks and guidelines; 2) thoughtful product design, especially regarding user interface decisions; 3) advancements in AI Ethics of powerful large models, including the development of better benchmarks and improved mitigation strategies.

Additionally, to address privacy concerns, methods exist for obfuscating or generating personal human attributes like faces (Yang et al., 2022a; Maximov et al., 2020), ensuring anonymity without compromising the quality of learned representations. While this avenue is worth exploring, it is currently beyond the scope of this paper.

In conclusion, Emu is presently a model intended for preliminary research purposes only, and deployment should be deferred until the aforementioned issues are thoroughly considered and addressed. Caution must be exercised before transitioning to production environments.

REFERENCES

Laion-aesthetics. `https://laion.ai/blog/laion-aesthetics/`, a.

Laion coco: 600m synthetic captions from laion2b-en. `https://laion.ai/blog/laion-coco/`, b.

Jean-Baptiste Alayrac, Jeff Donahue, Pauline Luc, Antoine Miech, Iain Barr, Yana Hasson, Karel Lenc, Arthur Mensch, Katherine Millican, Malcolm Reynolds, Roman Ring, Eliza Rutherford, Serkan Cabi, Tengda Han, Zhitao Gong, Sina Samangooei, Marianne Monteiro, Jacob L. Menick, Sebastian Borgeaud, Andy Brock, Aida Nematzadeh, Sahand Sharifzadeh, Mikolaj Binkowski, Ricardo Barreira, Oriol Vinyals, Andrew Zisserman, and Karén Simonyan. Flamingo: a visual language model for few-shot learning. In *NeurIPS*, 2022. URL http://papers.nips.cc/paper_files/paper/2022/hash/960a172bc7fbf0177ccccbb411a7d800-Abstract-Conference.html.

Anas Awadalla, Irena Gao, Joshua Gardner, Jack Hessel, Yusuf Hanafy, Wanrong Zhu, Kalyani Marathe, Yonatan Bitton, Samir Gadre, Jenia Jitsev, Simon Kornblith, Pang Wei Koh, Gabriel Ilharco, Mitchell Wortsman, and Ludwig Schmidt. Openflamingo, 2023. URL https://doi.org/10.5281/zenodo.7733589.

Max Bain, Arsha Nagrani, Gül Varol, and Andrew Zisserman. Frozen in time: A joint video and image encoder for end-to-end retrieval. In *Proceedings of the IEEE/CVF International Conference on Computer Vision*, pp. 1728–1738, 2021.

Tom Brown, Benjamin Mann, Nick Ryder, Melanie Subbiah, Jared D Kaplan, Prafulla Dhariwal, Arvind Neelakantan, Pranav Shyam, Girish Sastry, Amanda Askell, et al. Language models are few-shot learners. *Advances in neural information processing systems*, 33:1877–1901, 2020.

Delong Chen, Jianfeng Liu, Wenliang Dai, and Baoyuan Wang. Visual instruction tuning with polite flamingo. *arXiv preprint arXiv:2307.01003*, 2023a.

Keqin Chen, Zhao Zhang, Weili Zeng, Richong Zhang, Feng Zhu, and Rui Zhao. Shikra: Unleashing multimodal llm's referential dialogue magic. *arXiv preprint arXiv:2306.15195*, 2023b.

Xi Chen, Josip Djolonga, Piotr Padlewski, Basil Mustafa, Soravit Changpinyo, Jialin Wu, Carlos Riquelme Ruiz, Sebastian Goodman, Xiao Wang, Yi Tay, et al. Pali-x: On scaling up a multilingual vision and language model. *arXiv preprint arXiv:2305.18565*, 2023c.

Xinlei Chen, Hao Fang, Tsung-Yi Lin, Ramakrishna Vedantam, Saurabh Gupta, Piotr Dollár, and C Lawrence Zitnick. Microsoft coco captions: Data collection and evaluation server. *arXiv preprint arXiv:1504.00325*, 2015.

Yen-Chun Chen, Linjie Li, Licheng Yu, Ahmed El Kholy, Faisal Ahmed, Zhe Gan, Yu Cheng, and Jingjing Liu. UNITER: universal image-text representation learning. In Andrea Vedaldi, Horst Bischof, Thomas Brox, and Jan-Michael Frahm (eds.), *Computer Vision - ECCV 2020 - 16th European Conference, Glasgow, UK, August 23-28, 2020, Proceedings, Part XXX*, volume 12375 of *Lecture Notes in Computer Science*, pp. 104–120. Springer, 2020. doi: 10.1007/978-3-030-58577-8_7. URL https://doi.org/10.1007/978-3-030-58577-8_7.

Jaemin Cho, Jie Lei, Hao Tan, and Mohit Bansal. Unifying vision-and-language tasks via text generation. In Marina Meila and Tong Zhang (eds.), *Proceedings of the 38th International Conference on Machine Learning, ICML 2021, 18-24 July 2021, Virtual Event*, volume 139 of *Proceedings of Machine Learning Research*, pp. 1931–1942. PMLR, 2021. URL http://proceedings.mlr.press/v139/cho21a.html.

Aakanksha Chowdhery, Sharan Narang, Jacob Devlin, Maarten Bosma, Gaurav Mishra, Adam Roberts, Paul Barham, Hyung Won Chung, Charles Sutton, Sebastian Gehrmann, et al. Palm: Scaling language modeling with pathways. *arXiv preprint arXiv:2204.02311*, 2022.

Hyung Won Chung, Le Hou, Shayne Longpre, Barret Zoph, Yi Tay, William Fedus, Eric Li, Xuezhi Wang, Mostafa Dehghani, Siddhartha Brahma, et al. Scaling instruction-finetuned language models. *arXiv preprint arXiv:2210.11416*, 2022.

Wenliang Dai, Junnan Li, Dongxu Li, Anthony Meng Huat Tiong, Junqi Zhao, Weisheng Wang, Boyang Li, Pascale Fung, and Steven C. H. Hoi. Instructblip: Towards general-purpose vision-language models with instruction tuning. *CoRR*, abs/2305.06500, 2023. doi: 10.48550/arXiv.2305.06500. URL https://doi.org/10.48550/arXiv.2305.06500.

Abhishek Das, Satwik Kottur, Khushi Gupta, Avi Singh, Deshraj Yadav, José MF Moura, Devi Parikh, and Dhruv Batra. Visual dialog. In *Proceedings of the IEEE conference on computer vision and pattern recognition*, pp. 326–335, 2017.

Runpei Dong, Chunrui Han, Yuang Peng, Zekun Qi, Zheng Ge, Jinrong Yang, Liang Zhao, Jianjian Sun, Hongyu Zhou, Haoran Wei, et al. Dreamllm: Synergistic multimodal comprehension and creation. *arXiv preprint arXiv:2309.11499*, 2023.

Alexey Dosovitskiy, Lucas Beyer, Alexander Kolesnikov, Dirk Weissenborn, Xiaohua Zhai, Thomas Unterthiner, Mostafa Dehghani, Matthias Minderer, Georg Heigold, Sylvain Gelly, Jakob Uszkoreit, and Neil Houlsby. An image is worth 16x16 words: Transformers for image recognition at scale. In *9th International Conference on Learning Representations, ICLR 2021, Virtual Event, Austria, May 3-7, 2021*. OpenReview.net, 2021. URL https://openreview.net/forum?id=YicbFdNTTy.

Danny Driess, Fei Xia, Mehdi SM Sajjadi, Corey Lynch, Aakanksha Chowdhery, Brian Ichter, Ayzaan Wahid, Jonathan Tompson, Quan Vuong, Tianhe Yu, et al. Palm-e: An embodied multimodal language model. *arXiv preprint arXiv:2303.03378*, 2023.

Oran Gafni, Adam Polyak, Oron Ashual, Shelly Sheynin, Devi Parikh, and Yaniv Taigman. Make-a-scene: Scene-based text-to-image generation with human priors. In *European Conference on Computer Vision*, pp. 89–106. Springer, 2022.

Peng Gao, Jiaming Han, Renrui Zhang, Ziyi Lin, Shijie Geng, Aojun Zhou, Wei Zhang, Pan Lu, Conghui He, Xiangyu Yue, et al. Llama-adapter v2: Parameter-efficient visual instruction model. *arXiv preprint arXiv:2304.15010*, 2023.

Tao Gong, Chengqi Lyu, Shilong Zhang, Yudong Wang, Miao Zheng, Qian Zhao, Kuikun Liu, Wenwei Zhang, Ping Luo, and Kai Chen. Multimodal-gpt: A vision and language model for dialogue with humans. *arXiv preprint arXiv:2305.04790*, 2023.

Yash Goyal, Tejas Khot, Douglas Summers-Stay, Dhruv Batra, and Devi Parikh. Making the v in vqa matter: Elevating the role of image understanding in visual question answering. In *Proceedings of the IEEE conference on computer vision and pattern recognition*, pp. 6904–6913, 2017.

Danna Gurari, Qing Li, Abigale J Stangl, Anhong Guo, Chi Lin, Kristen Grauman, Jiebo Luo, and Jeffrey P Bigham. Vizwiz grand challenge: Answering visual questions from blind people. In *Proceedings of the IEEE conference on computer vision and pattern recognition*, pp. 3608–3617, 2018.

Yaru Hao, Haoyu Song, Li Dong, Shaohan Huang, Zewen Chi, Wenhui Wang, Shuming Ma, and Furu Wei. Language models are general-purpose interfaces. *arXiv preprint arXiv:2206.06336*, 2022.

Martin Heusel, Hubert Ramsauer, Thomas Unterthiner, Bernhard Nessler, and Sepp Hochreiter. Gans trained by a two time-scale update rule converge to a local nash equilibrium. *Advances in neural information processing systems*, 30, 2017.

Jonathan Ho and Tim Salimans. Classifier-free diffusion guidance. *arXiv preprint arXiv:2207.12598*, 2022.

Edward J. Hu, Yelong Shen, Phillip Wallis, Zeyuan Allen-Zhu, Yuanzhi Li, Shean Wang, Lu Wang, and Weizhu Chen. Lora: Low-rank adaptation of large language models. In *The Tenth International Conference on Learning Representations, ICLR 2022, Virtual Event, April 25-29, 2022*. OpenReview.net, 2022. URL `https://openreview.net/forum?id=nZeVKeeFYf9`.

Shaohan Huang, Li Dong, Wenhui Wang, Yaru Hao, Saksham Singhal, Shuming Ma, Tengchao Lv, Lei Cui, Owais Khan Mohammed, Qiang Liu, et al. Language is not all you need: Aligning perception with language models. *arXiv preprint arXiv:2302.14045*, 2023.

Chao Jia, Yinfei Yang, Ye Xia, Yi-Ting Chen, Zarana Parekh, Hieu Pham, Quoc V. Le, Yun-Hsuan Sung, Zhen Li, and Tom Duerig. Scaling up visual and vision-language representation learning with noisy text supervision. In Marina Meila and Tong Zhang (eds.), *Proceedings of the 38th International Conference on Machine Learning, ICML 2021, 18-24 July 2021, Virtual Event*, volume 139 of *Proceedings of Machine Learning Research*, pp. 4904–4916. PMLR, 2021. URL `http://proceedings.mlr.press/v139/jia21b.html`.

Wonjae Kim, Bokyung Son, and Ildoo Kim. Vilt: Vision-and-language transformer without convolution or region supervision. In Marina Meila and Tong Zhang (eds.), *Proceedings of the 38th International Conference on Machine Learning, ICML 2021, 18-24 July 2021, Virtual Event*, volume 139 of *Proceedings of Machine Learning Research*, pp. 5583–5594. PMLR, 2021. URL `http://proceedings.mlr.press/v139/kim21k.html`.

Jing Yu Koh, Daniel Fried, and Ruslan Salakhutdinov. Generating images with multimodal language models. *arXiv preprint arXiv:2305.17216*, 2023a.

Jing Yu Koh, Ruslan Salakhutdinov, and Daniel Fried. Grounding language models to images for multimodal inputs and outputs. In Andreas Krause, Emma Brunskill, Kyunghyun Cho, Barbara Engelhardt, Sivan Sabato, and Jonathan Scarlett (eds.), *International Conference on Machine Learning, ICML 2023, 23-29 July 2023, Honolulu, Hawaii, USA*, volume 202 of *Proceedings of Machine Learning Research*, pp. 17283–17300. PMLR, 2023b. URL `https://proceedings.mlr.press/v202/koh23a.html`.

Bo Li, Yuanhan Zhang, Liangyu Chen, Jinghao Wang, Jingkang Yang, and Ziwei Liu. Otter: A multi-modal model with in-context instruction tuning. *arXiv preprint arXiv:2305.03726*, 2023a.

Junnan Li, Ramprasaath R. Selvaraju, Akhilesh Gotmare, Shafiq R. Joty, Caiming Xiong, and Steven Chu-Hong Hoi. Align before fuse: Vision and language representation learning with momentum distillation. In Marc'Aurelio Ranzato, Alina Beygelzimer, Yann N. Dauphin, Percy Liang, and Jennifer Wortman Vaughan (eds.), *Advances in Neural Information Processing Systems 34: Annual Conference on Neural Information Processing Systems 2021, NeurIPS 2021, December 6-14, 2021, virtual*, pp. 9694–9705, 2021. URL https://proceedings.neurips.cc/paper/2021/hash/505259756244493872b7709a8a01b536-Abstract.html.

Junnan Li, Dongxu Li, Caiming Xiong, and Steven Hoi. Blip: Bootstrapping language-image pre-training for unified vision-language understanding and generation. In *International Conference on Machine Learning*, pp. 12888–12900. PMLR, 2022.

Junnan Li, Dongxu Li, Silvio Savarese, and Steven Hoi. Blip-2: Bootstrapping language-image pre-training with frozen image encoders and large language models. *arXiv preprint arXiv:2301.12597*, 2023b.

KunChang Li, Yinan He, Yi Wang, Yizhuo Li, Wenhai Wang, Ping Luo, Yali Wang, Limin Wang, and Yu Qiao. Videochat: Chat-centric video understanding. *arXiv preprint arXiv:2305.06355*, 2023c.

Tsung-Yi Lin, Michael Maire, Serge Belongie, James Hays, Pietro Perona, Deva Ramanan, Piotr Dollár, and C Lawrence Zitnick. Microsoft coco: Common objects in context. In *Computer Vision–ECCV 2014: 13th European Conference, Zurich, Switzerland, September 6-12, 2014, Proceedings, Part V 13*, pp. 740–755. Springer, 2014.

Fuxiao Liu, Kevin Lin, Linjie Li, Jianfeng Wang, Yaser Yacoob, and Lijuan Wang. Aligning large multi-modal model with robust instruction tuning. *arXiv preprint arXiv:2306.14565*, 2023a.

Haotian Liu, Chunyuan Li, Qingyang Wu, and Yong Jae Lee. Visual instruction tuning. *arXiv preprint arXiv:2304.08485*, 2023b.

Luping Liu, Yi Ren, Zhijie Lin, and Zhou Zhao. Pseudo numerical methods for diffusion models on manifolds. *arXiv preprint arXiv:2202.09778*, 2022.

Ilya Loshchilov and Frank Hutter. Decoupled weight decay regularization. *arXiv preprint arXiv:1711.05101*, 2017.

Jiasen Lu, Christopher Clark, Rowan Zellers, Roozbeh Mottaghi, and Aniruddha Kembhavi. Unified-io: A unified model for vision, language, and multi-modal tasks. *arXiv preprint arXiv:2206.08916*, 2022.

Yadong Lu, Chunyuan Li, Haotian Liu, Jianwei Yang, Jianfeng Gao, and Yelong Shen. An empirical study of scaling instruct-tuned large multimodal models. *arXiv preprint arXiv:2309.09958*, 2023.

Muhammad Maaz, Hanoona Rasheed, Salman Khan, and Fahad Shahbaz Khan. Video-chatgpt: Towards detailed video understanding via large vision and language models. *arXiv preprint arXiv:2306.05424*, 2023.

Kenneth Marino, Mohammad Rastegari, Ali Farhadi, and Roozbeh Mottaghi. Ok-vqa: A visual question answering benchmark requiring external knowledge. In *Proceedings of the IEEE/cvf conference on computer vision and pattern recognition*, pp. 3195–3204, 2019.

Maxim Maximov, Ismail Elezi, and Laura Leal-Taixé. Ciagan: Conditional identity anonymization generative adversarial networks. In *Proceedings of the IEEE/CVF conference on computer vision and pattern recognition*, pp. 5447–5456, 2020.

Seungwhan Moon, Andrea Madotto, Zhaojiang Lin, Tushar Nagarajan, Matt Smith, Shashank Jain, Chun-Fu Yeh, Prakash Murugesan, Peyman Heidari, Yue Liu, et al. Anymal: An efficient and scalable any-modality augmented language model. *arXiv preprint arXiv:2309.16058*, 2023.

Alex Nichol, Prafulla Dhariwal, Aditya Ramesh, Pranav Shyam, Pamela Mishkin, Bob McGrew, Ilya Sutskever, and Mark Chen. Glide: Towards photorealistic image generation and editing with text-guided diffusion models. *arXiv preprint arXiv:2112.10741*, 2021.

Long Ouyang, Jeffrey Wu, Xu Jiang, Diogo Almeida, Carroll Wainwright, Pamela Mishkin, Chong Zhang, Sandhini Agarwal, Katarina Slama, Alex Ray, et al. Training language models to follow instructions with human feedback. *Advances in Neural Information Processing Systems*, 35:27730–27744, 2022.

Alec Radford, Jong Wook Kim, Chris Hallacy, Aditya Ramesh, Gabriel Goh, Sandhini Agarwal, Girish Sastry, Amanda Askell, Pamela Mishkin, Jack Clark, Gretchen Krueger, and Ilya Sutskever. Learning transferable visual models from natural language supervision. In Marina Meila and Tong Zhang (eds.), *Proceedings of the 38th International Conference on Machine Learning, ICML 2021, 18-24 July 2021, Virtual Event*, volume 139 of *Proceedings of Machine Learning Research*, pp. 8748–8763. PMLR, 2021. URL http://proceedings.mlr.press/v139/radford21a.html.

Colin Raffel, Noam Shazeer, Adam Roberts, Katherine Lee, Sharan Narang, Michael Matena, Yanqi Zhou, Wei Li, and Peter J Liu. Exploring the limits of transfer learning with a unified text-to-text transformer. *The Journal of Machine Learning Research*, 21(1):5485–5551, 2020.

Aditya Ramesh, Mikhail Pavlov, Gabriel Goh, Scott Gray, Chelsea Voss, Alec Radford, Mark Chen, and Ilya Sutskever. Zero-shot text-to-image generation. In *International Conference on Machine Learning*, pp. 8821–8831. PMLR, 2021.

Aditya Ramesh, Prafulla Dhariwal, Alex Nichol, Casey Chu, and Mark Chen. Hierarchical text-conditional image generation with clip latents. *arXiv preprint arXiv:2204.06125*, 2022.

Robin Rombach, Andreas Blattmann, Dominik Lorenz, Patrick Esser, and Björn Ommer. High-resolution image synthesis with latent diffusion models. In *Proceedings of the IEEE/CVF Conference on Computer Vision and Pattern Recognition (CVPR)*, pp. 10684–10695, June 2022.

Chitwan Saharia, William Chan, Saurabh Saxena, Lala Li, Jay Whang, Emily L Denton, Kamyar Ghasemipour, Raphael Gontijo Lopes, Burcu Karagol Ayan, Tim Salimans, et al. Photorealistic text-to-image diffusion models with deep language understanding. *Advances in Neural Information Processing Systems*, 35:36479–36494, 2022.

Christoph Schuhmann, Romain Beaumont, Richard Vencu, Cade Gordon, Ross Wightman, Mehdi Cherti, Theo Coombes, Aarush Katta, Clayton Mullis, Mitchell Wortsman, et al. Laion-5b: An open large-scale dataset for training next generation image-text models. *arXiv preprint arXiv:2210.08402*, 2022.

John Schulman, Barret Zoph, Christina Kim, Jacob Hilton, Jacob Menick, Jiayi Weng, Juan Felipe Ceron Uribe, Liam Fedus, Luke Metz, Michael Pokorny, et al. Chatgpt: Optimizing language models for dialogue. *OpenAI blog*, 2022.

Quan Sun, Yuxin Fang, Ledell Wu, Xinlong Wang, and Yue Cao. Eva-clip: Improved training techniques for clip at scale. *arXiv preprint arXiv:2303.15389*, 2023.

Rohan Taori, Ishaan Gulrajani, Tianyi Zhang, Yann Dubois, Xuechen Li, Carlos Guestrin, Percy Liang, and Tatsunori B. Hashimoto. Stanford alpaca: An instruction-following llama model. `https://github.com/tatsu-lab/stanford_alpaca`, 2023.

Hugo Touvron, Thibaut Lavril, Gautier Izacard, Xavier Martinet, Marie-Anne Lachaux, Timothée Lacroix, Baptiste Rozière, Naman Goyal, Eric Hambro, Faisal Azhar, et al. Llama: Open and efficient foundation language models. *arXiv preprint arXiv:2302.13971*, 2023.

Ashish Vaswani, Noam Shazeer, Niki Parmar, Jakob Uszkoreit, Llion Jones, Aidan N Gomez, Łukasz Kaiser, and Illia Polosukhin. Attention is all you need. *Advances in neural information processing systems*, 30, 2017.

Ramakrishna Vedantam, C Lawrence Zitnick, and Devi Parikh. Cider: Consensus-based image description evaluation. In *Proceedings of the IEEE conference on computer vision and pattern recognition*, pp. 4566–4575, 2015.

Jianfeng Wang, Zhengyuan Yang, Xiaowei Hu, Linjie Li, Kevin Lin, Zhe Gan, Zicheng Liu, Ce Liu, and Lijuan Wang. Git: A generative image-to-text transformer for vision and language. *arXiv preprint arXiv:2205.14100*, 2022a.

Peng Wang, An Yang, Rui Men, Junyang Lin, Shuai Bai, Zhikang Li, Jianxin Ma, Chang Zhou, Jingren Zhou, and Hongxia Yang. Ofa: Unifying architectures, tasks, and modalities through a simple sequence-to-sequence learning framework. In *International Conference on Machine Learning*, pp. 23318–23340. PMLR, 2022b.

Yizhong Wang, Yeganeh Kordi, Swaroop Mishra, Alisa Liu, Noah A Smith, Daniel Khashabi, and Hannaneh Hajishirzi. Self-instruct: Aligning language model with self generated instructions. *arXiv preprint arXiv:2212.10560*, 2022c.

Zirui Wang, Jiahui Yu, Adams Wei Yu, Zihang Dai, Yulia Tsvetkov, and Yuan Cao. Simvlm: Simple visual language model pretraining with weak supervision. In *The Tenth International Conference on Learning Representations, ICLR 2022, Virtual Event, April 25-29, 2022*. OpenReview.net, 2022d. URL `https://openreview.net/forum?id=GUrhfTuf_3`.

Jason Wei, Maarten Bosma, Vincent Y. Zhao, Kelvin Guu, Adams Wei Yu, Brian Lester, Nan Du, Andrew M. Dai, and Quoc V. Le. Finetuned language models are zero-shot learners. In *The Tenth International Conference on Learning Representations, ICLR 2022, Virtual Event, April 25-29, 2022*. OpenReview.net, 2022. URL `https://openreview.net/forum?id=gEZrGCozdqR`.

Junbin Xiao, Xindi Shang, Angela Yao, and Tat-Seng Chua. Next-qa: Next phase of question-answering to explaining temporal actions. In *Proceedings of the IEEE/CVF Conference on Computer Vision and Pattern Recognition (CVPR)*, pp. 9777–9786, June 2021.

Dejing Xu, Zhou Zhao, Jun Xiao, Fei Wu, Hanwang Zhang, Xiangnan He, and Yueting Zhuang. Video question answering via gradually refined attention over appearance and motion. In *Proceedings of the 25th ACM international conference on Multimedia*, pp. 1645–1653, 2017.

Kaiyu Yang, Jacqueline H Yau, Li Fei-Fei, Jia Deng, and Olga Russakovsky. A study of face obfuscation in imagenet. In *International Conference on Machine Learning*, pp. 25313–25330. PMLR, 2022a.

Zhengyuan Yang, Zhe Gan, Jianfeng Wang, Xiaowei Hu, Yumao Lu, Zicheng Liu, and Lijuan Wang. An empirical study of gpt-3 for few-shot knowledge-based vqa. In *Proceedings of the AAAI Conference on Artificial Intelligence*, 2022b.

Qinghao Ye, Haiyang Xu, Guohai Xu, Jiabo Ye, Ming Yan, Yiyang Zhou, Junyang Wang, Anwen Hu, Pengcheng Shi, Yaya Shi, et al. mplug-owl: Modularization empowers large language models with multimodality. *arXiv preprint arXiv:2304.14178*, 2023.

Jiahui Yu, Zirui Wang, Vijay Vasudevan, Legg Yeung, Mojtaba Seyedhosseini, and Yonghui Wu. Coca: Contrastive captioners are image-text foundation models. *arXiv preprint arXiv:2205.01917*, 2022a.

Jiahui Yu, Yuanzhong Xu, Jing Yu Koh, Thang Luong, Gunjan Baid, Zirui Wang, Vijay Vasudevan, Alexander Ku, Yinfei Yang, Burcu Karagol Ayan, et al. Scaling autoregressive models for content-rich text-to-image generation. *arXiv preprint arXiv:2206.10789*, 2022b.

Lili Yu, Bowen Shi, Ramakanth Pasunuru, Benjamin Muller, Olga Golovneva, Tianlu Wang, Arun Babu, Binh Tang, Brian Karrer, Shelly Sheynin, et al. Scaling autoregressive multi-modal models: Pretraining and instruction tuning. *arXiv preprint arXiv:2309.02591*, 2023a.

Weihao Yu, Zhengyuan Yang, Linjie Li, Jianfeng Wang, Kevin Lin, Zicheng Liu, Xinchao Wang, and Lijuan Wang. Mm-vet: Evaluating large multimodal models for integrated capabilities. *arXiv preprint arXiv:2308.02490*, 2023b.

Rowan Zellers, Jiasen Lu, Ximing Lu, Youngjae Yu, Yanpeng Zhao, Mohammadreza Salehi, Aditya Kusupati, Jack Hessel, Ali Farhadi, and Yejin Choi. Merlot reserve: Neural script knowledge through vision and language and sound. In *Proceedings of the IEEE/CVF Conference on Computer Vision and Pattern Recognition*, pp. 16375–16387, 2022.

Yan Zeng, Hanbo Zhang, Jiani Zheng, Jiangnan Xia, Guoqiang Wei, Yang Wei, Yuchen Zhang, and Tao Kong. What matters in training a gpt4-style language model with multimodal inputs? *arXiv preprint arXiv:2307.02469*, 2023.

Lianmin Zheng, Wei-Lin Chiang, Ying Sheng, Siyuan Zhuang, Zhanghao Wu, Yonghao Zhuang, Zi Lin, Zhuohan Li, Dacheng Li, Eric. P Xing, Hao Zhang, Joseph E. Gonzalez, and Ion Stoica. Judging llm-as-a-judge with mt-bench and chatbot arena, 2023.

Deyao Zhu, Jun Chen, Xiaoqian Shen, Xiang Li, and Mohamed Elhoseiny. Minigpt-4: Enhancing vision-language understanding with advanced large language models. *arXiv preprint arXiv:2304.10592*, 2023a.

Wanrong Zhu, Jack Hessel, Anas Awadalla, Samir Yitzhak Gadre, Jesse Dodge, Alex Fang, Youngjae Yu, Ludwig Schmidt, William Yang Wang, and Yejin Choi. Multimodal c4: An open, billion-scale corpus of images interleaved with text. *arXiv preprint arXiv:2304.06939*, 2023b.

A Emu training

A.1 Pretraining

A.1.1 Dataset Details

Image-text Pairs. The LAION-2B dataset is the english subset of Laion-5B (Schuhmann et al., 2022) and contains large-scale image-text pairs data. LAION-COCO (lai, b) is captioned 600M images from LAION-2B with an ensemble of BLIP (Li et al., 2022) and CLIP (Radford et al., 2021) models. Whereas the text in LAION-COCO (lai, b) exhibits enhanced fluency and relevance to the associated images, it has insufficient text diversity and a potential loss of high-level semantic information, including world knowledge contents presented in the original LAION-2B dataset. Thus, we employ both the LAION-2B and LAION-COCO (lai, b) datasets during **Emu** pretraining.

Video-text Pairs. Webvid-10M (Bain et al., 2021) dataset contains a diversity of content with strong correlation between text and video. However, we found that a certain amount of the data contained irrelevant metadata information (*e.g.*resolution of the original video, camera parameters). To prevent the model from being influenced by these irrelevant details, we use heuristic rules to remove these content. Firstly, we build a word list consisting of irrelevant information. This word list is then utilized as a filtering mechanism to process the raw video text descriptions obtained from the original dataset. As a result, approximately 1 million datasets requiring cleaning are identified. Subsequently, specific rules are designed based on this list to identify and eliminate any words of irrelevant information within the text. Finally, the cleaned texts are subjected to rewriting using the Vicuna-13B (Zheng et al., 2023), thereby ensuring its fluency and enhancing the overall quality.

Interleaved Image and Text. Multimodal-C4 (Zhu et al., 2023b) is used as interleaved image-text data in pretraining. Following OpenFlamingo (Awadalla et al., 2023), we filter images based on CLIP similarity score to ensure the relevance of the images and text in each document. Specifically, any image with a CLIP similarity score below the threshold of 0.32 for all text in the same document is discarded. From each document, we sample a random subsequence of L = 1024 and take up to the first N = 5 images included in the sampled sequence. This process results in long text with the inclusion of multiple images. Additionally, we randomly sample N = 5 images along with their corresponding sentences to construct a subsequence of L = 512. This approach yields N = 5 image-text pairs.

Interleaved Video and Text. Videos with interleaved subtitles text represent a valuable and scalable source of multimodal data that has received limited attention thus far. In our study, we introduced YT-Storyboard-1B dataset, which collected storyboard images from *YouTube*, utilizing the video-ids provided by the YT-Temporal-1B dataset, which encompasses a vast collection of 18 million videos, equating to a total of 1.8 billion storyboard images. Specifically, for each video, we crawl the storyboard images and subtitles files directly. Where the sampling time between storyboard images is fixed, so the start time of each image can be determined by the order. Subtitle files record the content of each subtitle, as well as the start and end times. Therefore, storyboard images and subtitles can be sorted according to their timestamps and adjacent subtitles can be merged to form an interleaved video-text sequence. By opting to collect storyboard images instead of raw video data, we eliminate the necessity of video decoding. Moreover, this approach leads to a substantial 20-fold reduction in data storage costs, resulting in increased download efficiency.

A.1.2 Training Details

We report the detailed training hyperparameter settings of **Emu** during the pretraining in Table 5.

A.1.3 Ablations on Interleaved Video-text Data

We conduct ablation experiments to study the effectiveness of the YT-Storyboard-1B dataset. Smaller model size, batch size and shorter training schedule are used compared to the final **Emu** model to reduce the training cost. The model consists of a large-sized EVA-CLIP (Sun et al., 2023) as visual encoder and LLaMA-7B (Touvron et al., 2023) as multimodal modeling module. Image-text and video-text pairs are used as common datasets, including LAION-COCO (lai, b), LAION-2B (Schuhmann et al., 2022) and WebVid-10M (Bain et al., 2021), with batch size of 256, 256, 32, respectively. YT-Storyboard-1B batch size of 32 is used. Models are trained for 7.2k gradient steps on image-text and video-text pairs and additional 2.4k gradient steps on YT-Storyboard-1B.

Table 5: Summary of pretraining hyperparameters of **Emu**.

Configuration	**Emu** Pretraining
Vision encoder weight init.	EVA-CLIP (Sun et al., 2023)
Large language model weight init.	LLaMA-13B (Touvron et al., 2023)
Causal transformer weight init.	random init.
Vision encoder peak learning rate	4e-5
Large language model peak learning rate	3e-5
Causal transformer peak learning rate	1e-4
Warmup ratio	0.2
Learning rate schedule	cosine decay
Optimizer	AdamW (Loshchilov & Hutter, 2017)
Optimizer hyper-parameters	β_1, β_2, ϵ = 0.9, 0.98, 1e-6
Weight decay	0.05
Input image resolution	224×224
Iterations	10k
Data	LAION-2B (Schuhmann et al., 2022), LAION-COCO (lai, b), MMC4 (Zhu et al., 2023b), Webvid-10M (Bain et al., 2021), YT-Storyboard-1B (Zellers et al., 2022)
Batch size per dataset	128, 128, 64, 16, 16

Table 6: Quantitative comparison of w/wo interleaved video and text data during pre-training. k is the number of in-context examples, and we used the same example selection approach (*i.e.* RICES (Yang et al., 2022b)) as Flamingo (Alayrac et al., 2022). * indicates that the zero-shot prompt is built by using two examples from the task, where their corresponding images have been removed.

Setting	COCO	OKVQA		MSVDQA		MSRVTTQA	
	k=0	k=0 *	k=4	k=0 *	k=4	k=0 *	k=4
Emu-7B w/o YT-Storyboard-1B	110.8	**43.9**	44.6	30.2	31.1	16.9	19.9
Emu-7B w/ YT-Storyboard-1B	**112.9**	42.3	**45.7**	**30.8**	**34.9**	**17.9**	**20.8**

With YT-Storyboard-1B incorporated in the pretraining stage, Emu-7B achieves better zero-shot performance on MS-COCO (Chen et al., 2015), MSVDQA (Xu et al., 2017) and MSRVTTQA (Xu et al., 2017). Besides, YT-Storyboard-1B also brings stronger in-context learning capability under 4-shot evaluation.

A.2 VISUAL DECODING

A.2.1 DATASET DETAILS

LAION-Aesthetics (lai, a) is the subset of LAION-5B (Schuhmann et al., 2022) which have relatively high aesthetics quality while LAION-COCO (lai, b) has relatively high image-text correlation. To empower the visual decoder to possess the ability of decoding visual embeddings with both high quality and high relevance to text prompts, we use both LAION-COCO and LAION-Aesthetics for visual decoding training. More specifically, we filter all text prompts with length greater than 150 to preserve a large enough batch size and prevent the GPU memory overflow. This rule discards about 8% of LAION-Aesthetics and 0.01% of LAION-COCO data, which has little effect on data diversity.

A.2.2 TRAINING DETAILS

The detailed training setups are listed in Table 7.

Table 7: Summary of **Emu** visual decoder training hyperparameters.

Configuration	Visual Decoder
Weight init	Stable Diffusion v1.5
Batch size	$50 \times 4 \times 8$
Iterations	15k
Learning rate	warm up to 1e-4 for the first 5k, decrease to 5e-5 and 1e-5 at 10k and 14k
Input image resolution	512×512
Objective	ϵ-prediction
Optimizer	AdamW (Loshchilov & Hutter, 2017)
Optimizer hyper-parameters	β_1, β_2, ϵ = 0.9, 0.999, 1e-8
Weight decay	1e-2
Data	LAION-COCO (lai, b), LAION-Aesthetics (lai, a)
Data ratio	7:2

B Instruction Tuning

B.1 Dataset and Training Details

We collect publicly available language, image and video instruction datasets for instruction tuning.

- Language instructions: ShareGPT contains about 70K user dialogues with ChatGPT or GPT-4, and Alpaca (Taori et al., 2023) dataset contains 52K instruction-following data generated using self-instruct (Wang et al., 2022c) from OpenAI's `text-davinci-003`.
- Image instructions: we use LLaVA (Liu et al., 2023b) dataset consisting of three types of visual instructions, conversation, detailed description, and complex reasoning, with a total number of 158K image-text instruction-following samples. In our preliminary experiments, we found the instruction-tuned model often generates instruction-irrelevant detailed descriptions of the image. Thus, we remove the detailed description subset of LLaVA. We also find a bad pattern 'on top of the back of' in the model's response, and we filter all data that contains this pattern. The resulting 130K LLaVA subset is used for instruction tuning.
- Video instructions: we use VideoChat-11K (Li et al., 2023c) and a subset of Video-ChatGPT-100k (Maaz et al., 2023) as our video-instruction dataset. VideoChat-11K dataset is built from WebVid-10M consisting of 7K detailed video descriptions and 4K video conversations. Video-ChatGPT-100k is built from ActivityNet, and we sample an around 30K subset that includes only videos under one minute.

We use a batch size of 128 and train for 10K steps, with 3 epoches for ShareGPT, Alpaca and LLaVA datasets, and 60K samples for video-instruction data. The learning rate linearly warms up to 1e-5 in the first 500 steps, then decays to zero with a cosine schedule. The overall instruction tuning stage takes around 16 hours with 16 A100-80G GPUs. We attach LoRAs (Hu et al., 2022) on all linear projections of the self-attention layer, with the LoRA rank and alpha being 16.

B.2 System Messages

We use different system messages for language-instruction, image-instruction and video-instruction datasets, as shown in Table 8.

Table 8: Summary of the prompting template.

Task Type	<System Message>
Language Instruction Datasets	None
Image Instruction Datasets	`You are a helpful assistant and you will be presented with an image: [IMG]ImageContent[/IMG]. You will be able to see the image after I provide it to you. Please answer my questions based on the given image.`
Video Instruction Datasets	`You are a helpful assistant and you will be presented with a video consisting of multiple chronological images: [IMG]ImageContent[/IMG]. You will be able to see the video after I provide it to you. Please answer my questions based on the given video.`

Table 9: Summary of the evaluation benchmarks.

	Dataset	Task	Split	Metric
Image	COCO Text2Image	Text-to-Image Generation	Val	FID(↓)
	COCO Caption	Scene description	Test	CIDEr(↑)
	VQAv2	Scene understanding QA	Test-dev	VQA acc.(↑)
	OKVQA	External knowledge QA	Val	VQA acc.(↑)
	VizWiz	Scene understanding QA	Test-dev	VQA acc.(↑)
	VisDial	Image Dialogue	Val	NDCG(↑)
Video	MSVDQA	Event understanding QA	Test	Top-1 acc.(↑)
	MSRVTTQA	Event understanding QA	Test	Top-1 acc.(↑)
	NextQA	Temporal/Causal QA	Test	WUPS(↑)

C Evaluation

C.1 Benchmarks

Emu excels at performing diverse types of completion in multimodal sequences by accepting multimodal prompts, including text, images, videos, or their combinations, and generating comprehensive multimodal responses. To evaluate the capabilities of **Emu**, we conduct extensive benchmark tests covering various tasks, which are summarized in Table 9. Specifically, we meticulously select 9 benchmarks that encompass multimodal image/video and language tasks, including text-to-image generation, visual question answering for both images and videos, and image-based visual dialogue. When benchmarking OKVQA, we use VQAv2 evaluation code[3] and stem the answers using Porter stemming to consolidate answers following Marino et al. (2019). For other tasks, we either submit our results for evaluation on the official website or use standard evaluation code.

C.2 Zero-shot Evaluation

Prompt Template. To ensure that the model outputs answers in the required style for the benchmark tests, we prompt **Emu** and **Emu-I** with task-specific templates, as shown in Table 10. For each type of task, we have developed dedicated templates to structure the model's output. In these templates, "`{question}`" will be replaced with the question from the question-answering task, "`{history`

[3] `https://github.com/GT-Vision-Lab/VQA`

`question}`" will be replaced with the historical question from the multi-turn visual dialogues, and similarly "history answer" will be replaced with the historical annotated answer from the multi-turn visual dialogues. Then, the image/video will be added before the text as input to the model. Additionally, we implement post-processing techniques to filter out commonly occurring redundant phrases such as "it is", "it's", "a", "an", and "the". Furthermore, the model is required to output "unanswerable" for questions that cannot be answered in the VizWiz dataset. To achieve this, we augment the template by adding the phrase "`is the answer known?`" and prompt the model to respond with either "yes" or "no" by constraining the model generation. If the model responds with "no", we immediately return the answer as "unanswerable". On the other hand, if the model responds with "yes", we proceed to prompt the model to provide a valid answer.

Multimodal Chain-of-Thought Prompting. To enhance the capabilities of the pretrained model, we utilize the Multimodal Chain-of-Thought prompting technique. Initially, when presented with an image or video, we employ a prompt to guide the model in generating a descriptive caption. Subsequently, the model is given both the caption and a task-specific prompt to generate the final result. The complete prompt template is shown in Table 10, where the "`{caption}`" tag in template will be replaced with the descriptive text generated by **Emu**. The experimental results demonstrate that this test-time technique effectively improves the model's performance without any additional data, leveraging the inherent capability of the model itself.

Text-only Examples Prompting. To ensure a fair comparison with Flamingo, we include results obtained through text-only examples prompting, denoted by an asterisk (*) in Table 1. We adopt the same approach as Flamingo in selecting examples (*i.e., RICES*). This involves utilizing two text-only examples from the task as prompts, without any accompanying images (similar to the few-shot text prompts). During the evaluation process, we observed that this approach effectively formats the model's output, regardless of the label format of the datasets and the evaluation metrics employed, enabling a more accurate reflection of its true performance.

C.3 Few-shot Evaluation

In the few-shot evaluation settings, we incorporate a few example samples as prefixes in the template and connected the few-shot examples using "`.    `". Additionally, like Flamingo, we employ the Retrieval In-Context Example Selection (RICES) approach to select the few-shot examples.

To implement RICES, we begin by randomly selecting 5000 training set samples for each dataset. Then, using the pretrained EVA-CLIP model, we extract features from both the training set images/videos and the test set images/videos. For each test set sample, we select examples from the training set based on the highest cosine similarity using the extracted features, including them in the prompt. For the video-text task, we retrieve similar videos from the training set by comparing the mean of frame-level visual features extracted from our pretrained EVA-CLIP model.

Furthermore, we discover that the support video examples didn't require too many frames, which could exceed the LLM's context length limit. Therefore, we sample 8 frames for the given video and only 2 frames for the corresponding support video examples.

D Comparison with related work

The results are presented in Table 11, where **Emu** achieves state-of-the-art results on 5 out of 6 benchmarks evaluated.

CM3Leon Yu et al. (2023a) has similar motivation with us to train a unified image-to-text and text-to-image model. The most significant difference lies in that CM3Leon discretizes images, but we directly input and output image continuous features. We can find that CM3Leon performs much worse than **Emu** on image-to-text tasks.

AnyMAL Moon et al. (2023) is a large-scale Multimodal LLM that can process any modality, but have relatively weak performance on image to text tasks.

Table 10: Summary of the prompting template.

Model	Type	Template
Emu	Image Captioning	describing the image in detail. the image shows
	Image QA	a picture of {caption}. based on the picture, {question} short answer:
	Image Dialog	a picture of {caption}. based on the picture, {history question} short answer: {history answer}. ··· based on the picture, {question} short answer:
	Video Event understanding QA	a video of {caption}. a question about the video: {question} answer:
	Video Temporal/Causal QA	a video of {caption}. a question about the video: {question} short answer:
Emu-I	Image Captioning	[USER]: please provide an accurate and concise description of the given image. [ASSISTANT]: the image depicts a photo of
	Image QA	[USER]: based on the content of the image and common sense, please provide an accurate answer consisting of only one word or phrase. [ASSISTANT]: the answer is:
	Image Dialog	[USER]: {history question} [ASSISTANT]: {history answer}.<\s> ··· [USER]: {question} [ASSISTANT]:
	Video Event understanding QA	[USER]: based on the content of the video and common sense, please provide an accurate answer consisting of only one word or phrase. {question} [ASSISTANT]: the answer is:
	Video Temporal/Causal QA	[USER]: based on the content of the video and common sense, please provide an accurate short answer. {question} [ASSISTANT]: the answer is:

Table 11: Zero-shot comparison with concurrent work.

Models	COCO (Image2Text)	COCO (Text2Image)	VQAv2	OKVQA	VizWiz	VisDial
CM3Leon	61.6	**10.82**	47.6	23.8	37.6	22.6
AnyMAL-13B	99.5	-	59.6	33.1	24.4	-
Emu	112.4	11.66	52.0	38.2	34.2	47.4
Emu *	-	-	52.9	42.8	34.4	47.8
Emu-I	**120.4**	-	57.2	43.4	32.2	43.0
Emu-I *	-	-	**62.0**	**49.2**	**38.3**	**51.1**

E QUALITATIVE CASES

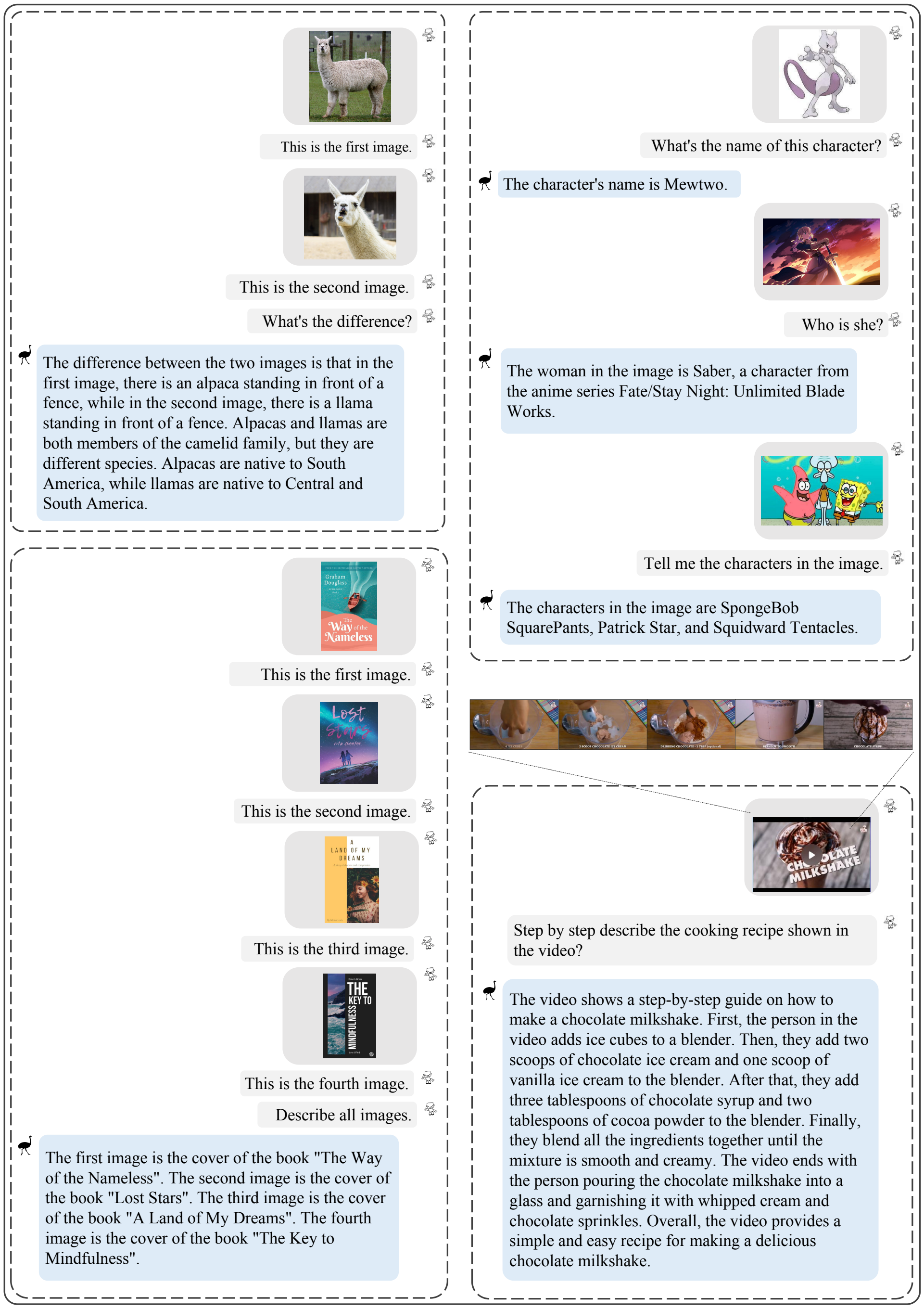

Figure 4: Examples of interleaved multi-image understanding(left side), real-world knowledge grounding(upper right), detailed video understanding(lower right).

Mahatma Gandhi Spinning Yarn in the Late 1920s

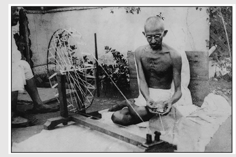

What does the image show? Describe all details including the figures, texts and numbers.

The image shows a black and white photograph of Mahatma Gandhi spinning yarn in the late 1920s. Gandhi is sitting on the ground with a spinning wheel in front of him. He is wearing a white shawl and appears to be focused on spinning the yarn. There are no other figures or objects visible in the image.

Explain this meme to me.

This meme features a cat with its mouth open and the caption "This is your face when a teacher gives you a surprise test." The meme is meant to be humorous and is often used to express frustration or annoyance with unexpected situations.

Where is it in the image?

The image shows the Twelve Apostles on the Great Ocean Road in Victoria, Australia.

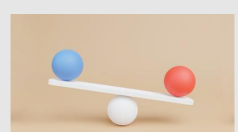

Which ball is heavier?

The red ball is heavier than the blue ball.

Figure 5: Examples of multimodal assistant.

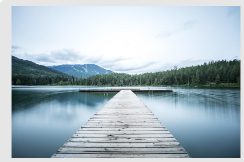

What are the things I should be cautious about when I visit here?

There are a few things you should be cautious about when visiting the lake:
1. Weather: The weather at the lake can be unpredictable, with sudden changes in temperature, wind, and precipitation. Make sure to check the weather forecast before your visit and pack appropriate clothing and gear.
2. Wildlife: The lake is home to a variety of wildlife, including bears, wolves, and moose. Make sure to stay on designated trails and keep your distance from any wildlife you encounter.
3. Water quality: The lake's water quality can vary depending on the time of year and the weather conditions. Make sure to check with local authorities before swimming or boating in the lake to ensure it is safe to do so.
4. Navigation: The lake is large and can be difficult to navigate, especially for inexperienced boaters. Make sure to familiarize yourself with the lake's layout and any potential hazards before venturing out on the water.
5. Safety equipment: Make sure to bring any necessary safety equipment, such as life jackets, first aid kits, and communication devices, in case of emergencies.

By taking these precautions, you can ensure a safe and enjoyable visit to the lake.

Do you have any suggestions about safety equipment?

Yes, here are a few suggestions for safety equipment:
1. Life jackets: Make sure to bring a life jacket for each person in your group, especially if you plan on boating or swimming in the lake.
2. First aid kit: A well-stocked first aid kit can be a lifesaver in case of emergencies. Make sure to include items such as bandages, antiseptic wipes, and pain relievers.
3. Communication devices: Bring a reliable communication device, such as a cell phone or walkie-talkie, in case of emergencies.
4. Navigation equipment: If you plan on boating or kayaking in the lake, make sure to bring a map, compass, and GPS device to help you navigate the waters.

By bringing these safety equipment, you can ensure a safe and enjoyable visit to the lake.

Can you write a poem about the image?

Sure, here's a poem about the image:
The serene lake stretches out before me,
A vast expanse of crystal-clear water.
The sun shines down, casting a golden glow,
As I take in the breathtaking view.
The gentle waves lap against the shore,
Creating a soothing symphony of sound.
I feel a sense of peace and tranquility,
As I bask in the beauty of this place.

Figure 6: Examples of multi-turn dialogue.

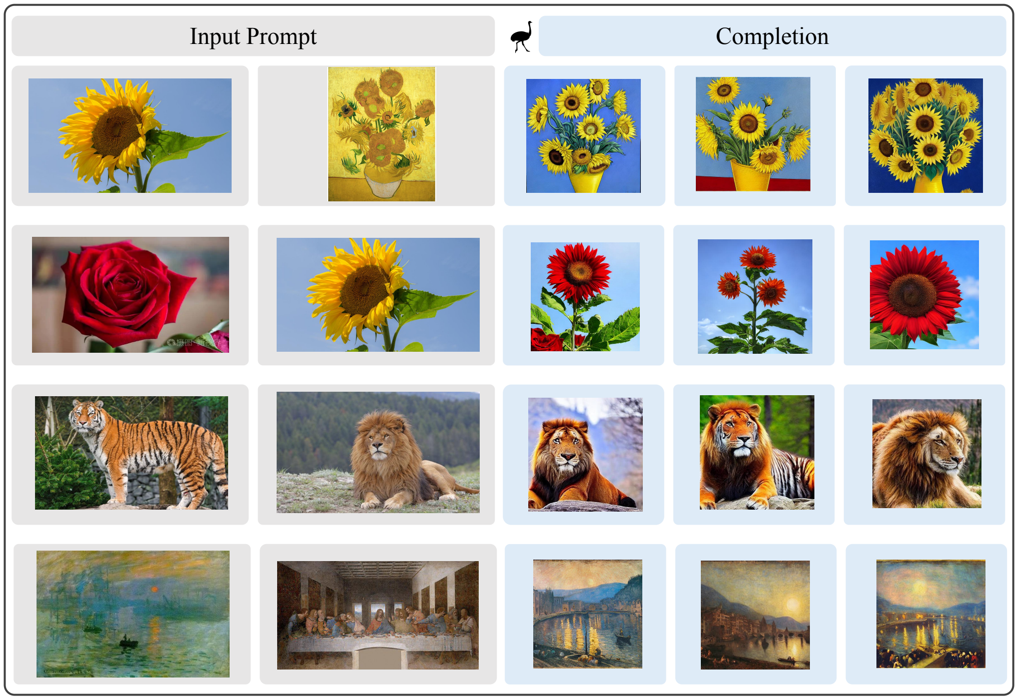

Figure 7: Examples of image blending.

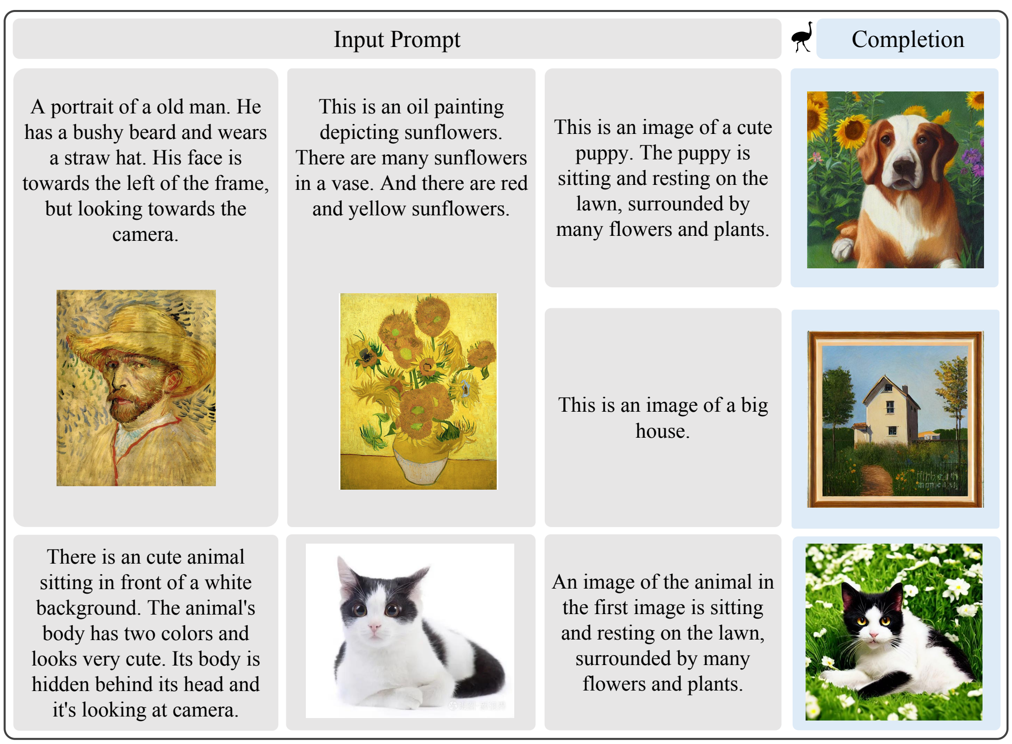

Figure 8: Examples of in-context text-to-image generation.

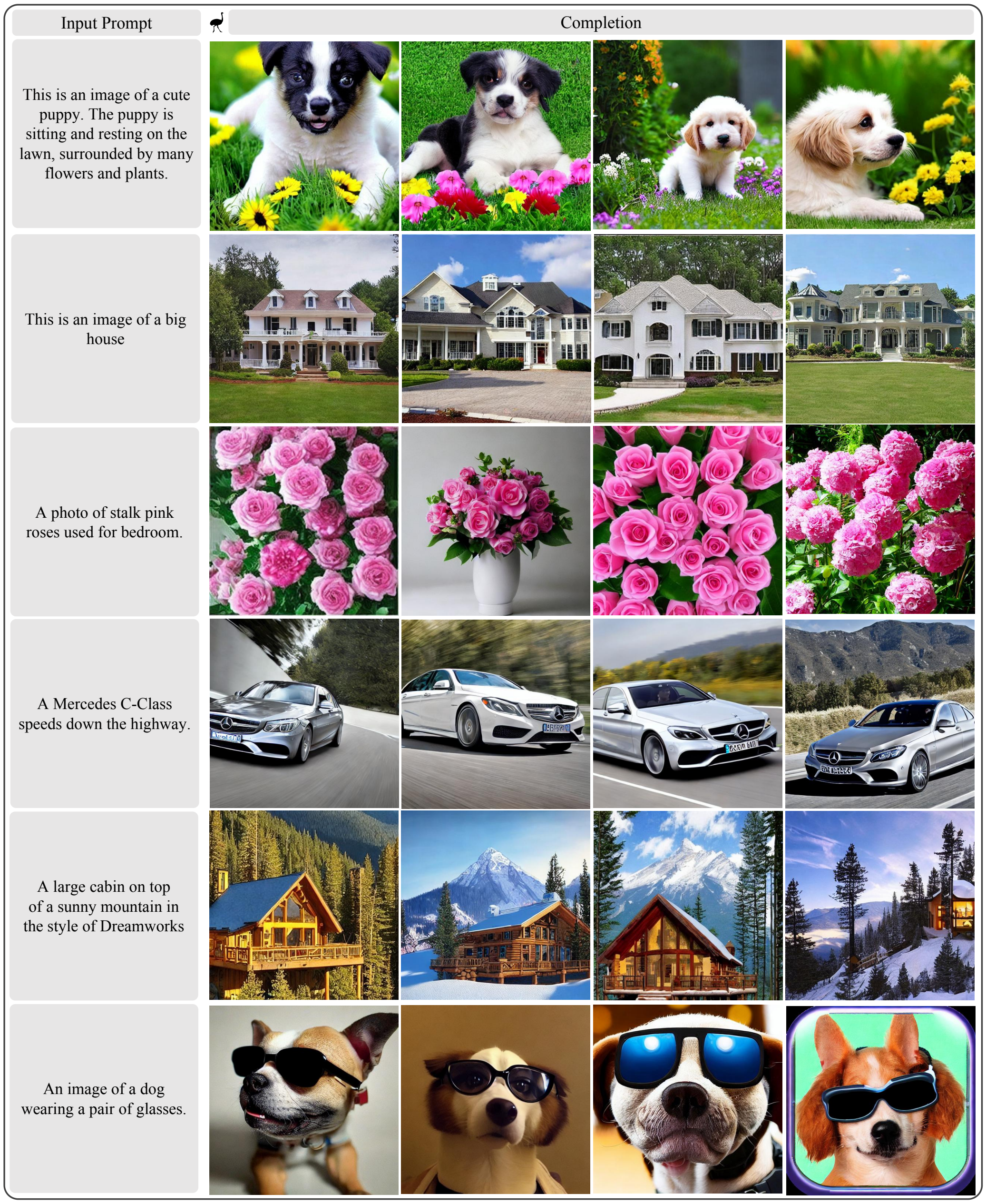

Figure 9: Examples of text-to-image generation.

Input Image

Input Text

Describe the image in detail.

Model Output

Emu

The image is a painting by Claude Monet titled "Impression, Sunrise". It depicts a serene scene of the sun rising over the water. The painting is done in a loose, impressionistic style, with visible brushstrokes and a focus on capturing the essence of the scene rather than the details. The colors are muted and soft, with shades of blue, pink, and yellow dominating the canvas.

In the foreground of the painting, there is a small boat bobbing up and down on the water. The sun is just peeking over the horizon, casting a warm, golden light over the scene. The water is calm and still, reflecting the colors of the sky above.

In the background of the painting, there are a few buildings visible, but they are mostly obscured by the mist and haze of the early morning. The sky is a mix of pink and blue, with a few wispy clouds drifting lazily across the sky.

Overall, the painting is a beautiful and serene depiction of a peaceful morning on the water. The soft colors and loose brushstrokes evoke a sense of calm and tranquility, inviting the viewer to take a moment to appreciate the beauty of nature.

LLaVA

The image is a captivating scene of a small boat floating on a body of water, possibly a bay or a river, during a beautiful sunset. The boat is positioned towards the center of the picture, surrounded by a serene atmosphere.

There are several other boats scattered throughout the image, some closer to the edges of the frame, while others are positioned more towards the center. The presence of multiple boats adds a sense of depth and interest to the scene.

The sunset casts a warm glow on the water and the boats, creating a picturesque and tranquil environment for those on the small boats to enjoy the view.

mPLUG-Owl

The painting depicts a beautiful sunrise over the ocean, creating a stunning and serene atmosphere. The scene is set against a backdrop of a blue-gray sky, with a bright yellow sun peeking out from behind a cloud.

The water in the foreground of the painting is calm and peaceful, gently reflecting the sun's rays. Several sailboats can be seen floating in various positions, adding to the tranquil atmosphere of this early morning moment. In addition to boats, there are several birds flying in different directions, enjoying the beautiful view.

InstructBLIP

In this painting, Claude Monet's famous impressionist artwork titled "Sunrise" takes center stage. The painting depicts the beautiful sunrise over the horizon, with its warm orange and yellow hues spreading across the sky. The water is also a significant part of the painting, with several boats sailing along it. The sunrise is captured in the middle of the painting, with boats scattered across the scene. In the background, the boats and the water are surrounded by various colors, with some areas featuring a lighter, brighter tone. The sunrise creates a serene and peaceful atmosphere, while the boats add a touch of activity to the scene.

Figure 10: Comparison of **Emu** with other methods on **image captioning task**.

Input Image

Input Text Tell me 8 books written by the woman and recommend one to me.

Model Output

Emu

Here are 8 books written by Agatha Christie:

1. "The Mysterious Affair at Styles" (1920)
2. "The Secret Adversary" (1922)
3. "The Murder on the Links" (1923)
4. "The Man in the Brown Suit" (1924)
5. "The Secret of Chimneys" (1925)
6. "The Murder of Roger Ackroyd" (1926)
7. "The Big Four" (1927)
8. "The Murder at the Vicarage" (1930)

Recommendation: "The Murder of Roger Ackroyd" (1926)

"The Murder of Roger Ackroyd" is considered by many to be Agatha Christie's greatest mystery novel. It is a classic whodunit with a twist ending that will keep you guessing until the very end.

LLaVA

The woman in the image, Agatha Christie, has written numerous books, totaling up to 66 novels, including mysteries and thrillers. One of her most famous and highly recommended books is "And Then There Were None." This book is a classic whodunit novel that tells the story of ten strangers who are lured to an isolated island and then murdered one by one, according to the rules of the famous nursery rhyme. The intricate plot, unique setting, and engaging characters make it an excellent read for anyone who enjoys mysteries and suspense.

mPLUG-Owl

Agatha Christie was a prolific British author who wrote over 80 novels, short stories, and plays. Some of her most famous works include:

1. Murder on the Orient Express (1934): A classic mystery novel about the investigation of a murder on a luxury train.
2. And Then There Were None (also known as Ten Little Indians) (10 Little Indian, 2015)
3. The Murders on The Rue Morgue (first published in 90s) - A detective story about a series of murders in Paris.
4. A MurDER IS ANNOUNCED (published in the 40's). A play that was adapted for a movie and later became a TV mini-series. It'll give you a glimpse into her writing style.

InstructBLIP

the spiderwick chronicles

Figure 11: Comparison of **Emu** with other methods in term of **following human instructions**.

Input Video

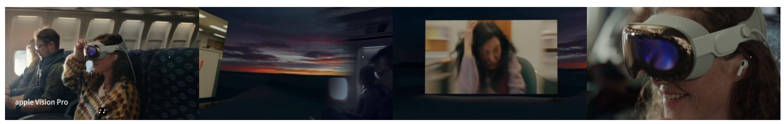

Input Text: What's the woman doing in the video?

Model Output

Emu: The woman in the video is wearing a pair of Apple VR goggles while sitting in an airplane. She appears to be using the goggles to watch something, possibly a video or a 360-degree view of the airplane's surroundings.

Video-ChatGPT: The woman is sitting in a plane and looking out of the window.

ImageBind-LLM: The woman is looking at her cell phone, possibly using it to take a picture or view something on the screen.

Figure 12: Comparison of **Emu** with other methods in term of **following human instructions**.